Journal of Physical Science, Vol. 30(2), 21–35, 2019

First-principles Electronic Study of Metal-insulator Transition in the Rutile CrO_2 at Room Temperature

Sarajit Biswas

Department of Physics, Taki Government College, Taki,
North 24 Parganas-743429, West Bengal, India

E-mail: srisabuj.phys@gmail.com

Published online: 25 August 2019

To cite this article: Biswas, S. (2019). First-principles electronic study of metal-insulator transition in the rutile CrO_2 at room temperature. *J. Phys. Sci.*, 30(2), 21–35, https://doi.org/10.21315/jps2019.30.2.2

To link to this article: https://doi.org/10.21315/jps2019.30.2.2

ABSTRACT: *First-principles electronic structure calculations were employed for the electronic, magnetic and structural properties of rutile CrO_2. This material is a ferromagnetic half-metal with a semiconducting gap of 1.85 eV. The sharing of a single electron by Cr-3d_{yz} and d_{xz} orbitals is responsible for the metallic behaviour of CrO_2 for the majority spin channel. For the application of on-site Coulomb interaction U up to 4 eV, the electrons in the valence band polarise towards the Fermi level (E_F), while the electrons in the conduction band polarise away from E_F. The enhanced shifting of conduction bands of the spin minority channel is responsible for the augmentation of the semiconducting spin gap. This system undergoes a metal-insulator transition (MIT) upon the application of U = 5 eV. Due to the presence of electron correlation, the electron in the d_{xy} orbital shifts well below E_F, while bonding components of d_{yz} and d_{xz} orbitals are occupied by the remaining single electron. Nevertheless, anti-bonding components of these two states remain unoccupied. Consequently, a band gap of $E_g \sim 0.2$ eV is opened near E_F. The double exchange interactions between the partially occupied Cr-t_{2g} states and p-d hybridisations are responsible for the ferromagnetic behaviour of CrO_2 in both half-metallic and insulating phases.*

Keywords: Rutile, crystal structure of CrO_2, metal-insulator transition, Coulomb repulsion, First-principles electronic calculations

1. INTRODUCTION

CrO_2 has recently attracted increasing interest due to its unusual electronic and magnetic properties.[1–5] The present compound is metallic for the spin majority

carriers and is insulating for the spin minority carriers. Therefore, this material exhibits half-metallic (HM) behaviour. This exceptional HM behaviour of CrO_2 has attracted a great attention in current years, both in theoretical and experimental regimes.[6–15] Under ambient conditions, this compound crystallises in the tetragonal structure (space group $P4_2/mnm$) of rutile type exhibiting half-metallic ferromagnetic (HMF) behaviour with a very high Tc ≈ 390 K compared to other transition metal oxides (TMOs). These two properties along with its wide availability in nature make CrO_2 significantly and technologically important and ideal material for developing spintronic devices.[16–18] Additionally, CrO_2 turns into a very suitable and promising material for applications in devices based on tunnelling magneto-resistance with a favourable switching behaviour at small fields[4,19,20] and intergrain-tunnelling magneto-resistance due to its HM property.[21,22] The Cr atoms in CrO_2 have formal valence 4+ (Cr^{4+}), hence two 3d ($3d^2$) electrons in the t_{2g} symmetry, while the e_g states remain empty. Therefore, one would expect the manifestation of the correlation effect of the Mott-Hubbard nature.

The most important and controversial issue is the role of on-site Coulomb correlation. Although most of the theoretical calculations based on the local spin density approximation (LSDA) correctly predicted the half-metallic ground state of CrO_2. In spite of this, the LSDA method is well known to be unable to determine the proper electronic properties of 3d metal oxides due to insufficient treatment of Coulomb correlations. In this respect, the LSDA+U method which includes explicitly an on-site Coulomb correlation term (U) can be employed for improvement in the description of ground state properties of most of the 3d metal oxides because it correctly accounts for the insulating ground state.

In the present work, the ground state properties of CrO_2 in its rutile phase are investigated, both in LSDA and LSDA+U schemes. In the LSDA calculations, the system exhibits HMF behaviour, but dramatic changes in the electronic properties were observed whenever Coulomb correlation U is applied (LSDA+U calculations). This compound remains in its HMF phase up to U = 4 eV. Eventually, this material encounters a metal-insulator transition (MIT) at U = 5 eV, preserving ferromagnetism (FM). The FM in the insulating phase is very unusual; because FM is associated with metals and antiferromagnetism (AFM) goes hand in hand with an insulator. In this paper, the origin of MIT in CrO_2 has been investigated comprehensively.

2. METHOD OF CALCULATIONS

The total energy, band structure, densities of states (DOS) and structural analysis of rutile CrO_2 are carried out using density functional theory (DFT) as implemented

in the tight-binding linear muffin-tin orbital (TB-LMTO) method in its atomic sphere approximation (ASA).[23–27] LSDA and LSDA+U with inclusion of Hubbard type Coulomb correlation U were adopted for the electronic structure calculations of CrO_2.[28] Self-consistent, fully spin-polarised electronic structure calculations were performed after the full-relaxation of internal atomic positions and lattice parameters. The rutile structure is stable at ambient pressure and has a simple tetragonal (space group $P4_2/mnm$). The Bravais lattice consists of two formula units (f.u.) per unit cell. In the FM ground state, the lattice parameters used were a = b = 4.422A° and c = 2.917A°. The Cr atom is located at (0, 0, 0) and O atom is positioned at (u, u, 0) with u = 0.302.[29] Since LMTO method gives accurate results for closely packed structure, and the structures under consideration are loosely packed, hence it is required to introduce empty spheres within the unit cell without hampering crystal symmetry. For this goal, two empty spheres E and E1 were introduced. The calculated muffin-tin radii (R_{MT}) for Cr, O, E and E1 were 2.30A°, 1.86A°, 1.82A° and 1.66A°, respectively.

3. RESULTS AND DISCUSSION

3.1 DOS Calculations

The FM spin-polarised electronic structure calculations were carried out in the investigation of the electronic and magnetic properties of rutile CrO_2. The total ground state energy, effective and individual magnetic moments of Cr and O, DOS and band structure of the present material have been performed for both LSDA and LSDA+U formalisms. The first motivation in this direction was to calculate the DOS of rutile CrO_2 using the LSDA scheme. Figure 1 provides the total, Cr-3d and O-2p DOS calculated by the LSDA method. The system is found metallic in the spin majority channel, whereas it is insulating in the down spin channel with a semiconducting spin gap of $E_g \sim 1.85$ eV. Considering both spin channels, the system is thereby half-metallic. It is obvious from this figure that the DOS in the close vicinity of E_F is predominated by the Cr-3d character. The octahedral crystal field splits Cr-3d manifold into triply degenerate t_{2g} and doubly degenerate e_g bands. It is unambiguous from Figure 1 that the t_{2g} and e_g bands are well separated from each other in both spin channels, which indicates 100% spin polarisation. The t_{2g} and e_g bands are observed in the energy spectrum of –1.3 eV to 1.07 eV and 1.34 eV to 4.50 eV respectively; with a spin gap of ($\Delta\uparrow$) ~ 0.27 eV between them. In the down spin channel, these two bands are found in the energy range of 0.35 eV to 2.6 eV and 3.1 eV to 6.1 eV respectively; having a spin gap of ($\Delta\downarrow$) ~ 0.5 eV.

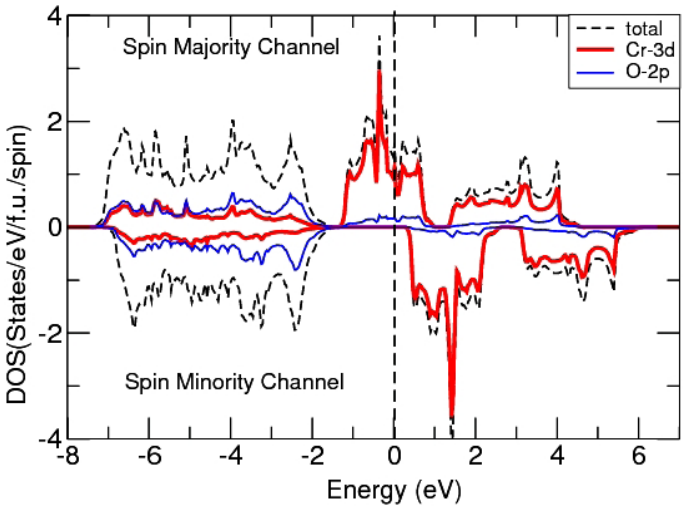

Figure 1: Calculated total, Cr-3d and O-2p DOS in the LSDA calculations. The spin majority channel is metallic, whereas the spin minority channel is insulating with a semiconducting gap of $E_g \sim 1.85$ eV.

For the spin majority channel, the available two Cr-3d electrons are distributed among the three t_{2g} states in such a manner that the occupied states are downshifted below E_F and partially occupied states are found near E_F. Nevertheless, the two e_g states are found empty and are pushed above E_F. The scenario is dissimilar in the spin minority channel. In this channel, the entire Cr-3d bands are identified above E_F. It is noteworthy from Figure 1 that the energy windows –7.24 eV to –1.6 eV and –7.07 eV to –1.54 eV are dominated by O-2p bands respectively for the up and down spin channels. It is also clear that O-2p orbitals are hybridised with Cr-3d orbitals that are accounted for the FM behaviour of CrO_2.

Since the LSDA method is incapable to predict the exact ground state properties of most of the TMOs, because it does not account electron correlations, therefore on-site Coulomb repulsion U is applied in the LSDA+U formalism to correct the electron correlations and hence to predict the exact ground state properties of CrO_2. Consequently, electron correlation effects on the electronic and magnetic properties of CrO_2 are also accounted. In this direction, a series of U starting from 1 eV to 6 eV were successively applied to the system. It is revealed from this study that the system remains in its HMF phase up to U = 4 eV, although the semiconducting band gaps and p-d hybridisations gradually enhance with U. Eventually, the system encounters MIT upon the application of U = 5 eV, preserving its ferromagnetism in the insulating phase. Further increase of U widens the band gap. This MIT in CrO_2, even in the rutile phase at ambient condition is very interesting, because only

pressure induced or V-doped MIT is observed in CrO_2 systems.[30–32] Accordingly, the ferromagnetism in the insulating phase of CrO_2 is unusual since it is associated with metals and AFM goes hand in hand with insulating TMOs. Therefore, the investigation of the ferromagnetic insulating (FI) behaviour of CrO_2 in the HT rutile phase is extremely exciting to be carried out.

The first dedication in this line was to understand the effect of Coulomb repulsion U in the range of 1 eV to 6 eV. The calculated total densities of states (TDOS) of CrO_2 for different U values are shown in Figure 2. It is noticeable from this figure that the semiconducting band gap increases up to U = 4 eV. The semiconducting band gaps identified for U = 1 eV to 4 eV are 1.87 eV, 2.19 eV, 2.39 eV and 2.56 eV, respectively. It is also obvious from Figure 2 that the energy bands are shifted towards E_F in the valence bands and are shifted away from E_F in the conduction bands with the augmentation of U. The Fermi level is found in the deep valley of a pseudogap, from which one can anticipate that only a minor change in the crystal symmetry can modify its electronic and magnetic properties. This can be achieved by applying Coulomb interaction U to the system. With the increase of U (up to 4 eV) the depth of the pseudogap enhances, and finally, for U = 5 eV, a band gap of $E_g \sim 0.2$ eV is opened near the close vicinity of E_F. Therefore, until and unless U = 5 eV is applied, the system remains in its HMF phase. Nevertheless, the band gap computed for U = 6 eV is 0.6 eV. Therefore, applications of higher U values widen the band gaps.

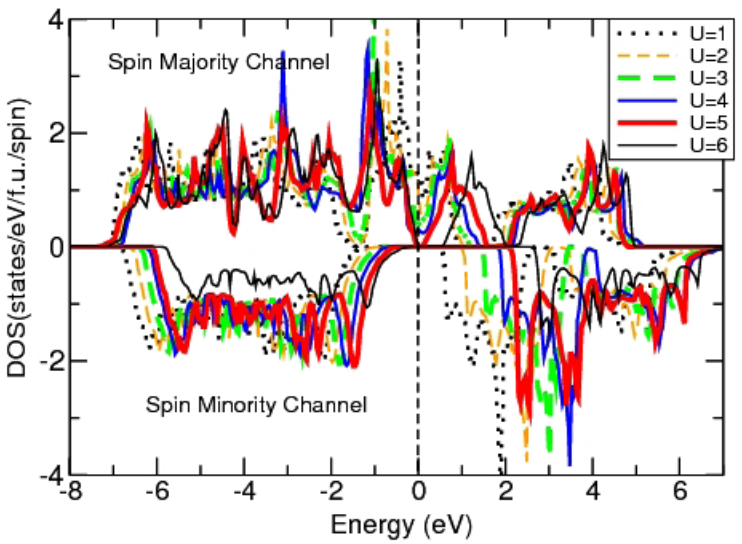

Figure 2: Calculated TDOS in the LSDA+U calculations for different U values starting from 0 to 6 eV. The system remains half-metallic up to U = 4 eV and undergoes MIT at U = 5 eV.

The calculated total ground state energies and magnetic moments are reported in Table 1. It is plain from this table that the ground state energy enhances upon the application of U due to increase in the repulsive electrostatic force which comes out from strong Cr-3d electron correlation effects. These electron-correlations are consequently crucial for MIT in rutile CrO_2. The calculated TDOS of Cr-3d bands at E_F and the number of Cr-3d electrons are embedded in Table 2. It is clear from this table that the number of Cr-3d electrons and hence TDOS increase with U for the spin-up channel, while reduces for the spin-down channel. The calculated TDOS and number of Cr-3d electrons for all the Cr-sites are found the same. Hence, no charge ordering/transfer is responsible for the observed MIT.

Table 1: Calculated total ground state energies (E_T), effective magnetic moments (μ_{eff}), Cr and O-magnetic moments (μ_{Cr} and μ_O) and band gaps (E_g) for different U values. O-sites are anti-coupled with Cr-sites as magnetic moments of O-sites are in opposite directions to that of Cr-sites.

Value of U	E_T (eV)	μ_{eff} (μ_B)	μ_{Cr} (μ_B)	μ_O (μ_B)	E_g (eV)
0	–4796.94	–4.0	–2.0	+0.04	0
1	–4796.92	–4.0	–2.0	+0.03	0
2	–4796.81	–4.0	–2.06	+0.07	0
3	–4796.69	–4.0	–2.10	+0.10	0
4	–4796.57	–4.0	–2.12	+0.12	0
5	–4796.15	–4.0	–2.14	+0.13	0.2
6	–4796.10	–4.0	–2.16	+0.15	0.6

Table 2: Calculated TDOS of the Cr-3d bands at E_F and number of Cr-3d electrons for different U values.

Values of U (eV)	TDOS (states/eV/spin/f.u.)		No. of electrons	
	up spin (↑)	down spin (↓)	up spin (↑)	down spin (↓)
0	2.84	0.92	2.85	0.88
1	2.82	0.90	2.84	0.88
2	2.86	0.90	2.87	0.87
3	2.89	0.87	2.89	0.80
4	2.86	0.81	2.90	0.77
5	2.77	0.83	2.83	0.79
6	2.77	0.81	2.83	0.76

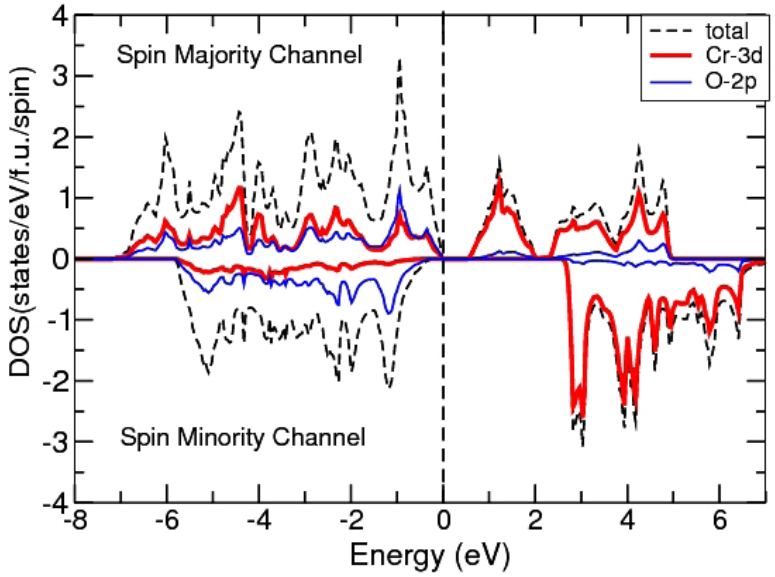

Figure 3: Calculated total, Cr-3d and O-2p DOS in the LSDA+U treatment with U = 6 eV. The system is insulating with a band gap $E_g \sim 0.6$ eV.

To understand what exactly happens in the MIT of rutile CrO_2 upon the application of higher U values (U > 4 eV), the DOS are also calculated for higher U values. The total, Cr-3d and O-2p DOS are represented in Figure 3 by employing U = 6 eV. Such higher Coulomb interaction is utilised for the better realisation of DOS and band structures. It is evident from this figure that the Cr-3dt_{2g} bands break into two energy bands for the spin-up channel. The first one is found in the energy range –7.0 eV to 0 eV that is occupied, while the other is found in the energy range of 0.6 eV to 2.0 eV that is unoccupied. The e_g bands remain empty and are found in the energy spectrum 2.36 eV to 5.0 eV. Consequently, a band gap of 0.6 eV is identified in this channel. The spin minority channel remains insulating. The unoccupied t_{2g} and e_g bands are found far above E_F and hence no spin gap is observed due to high spin polarisation. It is also evident from Figure 3 that O-2p orbitals are strongly hybridised with occupied Cr-3d orbitals. This enhanced p-d hybridisation is responsible for the increase in the strength of ferromagnetism of CrO_2.

3.2 Band Structure Calculations

To elucidate the origin of the MIT in rutile CrO_2 at room temperature (RT), the partial band structure (PBS) calculations were carried out extensively. The first enthusiasm in this line was to investigate the PBS of Cr-3d and O-2p orbitals in

the absence of U. Due to the presence of octahedral crystal field, triply degenerate Cr-3dt_{2g} bands split into d_{xy}, d_{yz} and d_{xz} states, while doubly degenerate e_g bands split into $d_{x^2-y^2}$ and $d_{3z^2-r^2}$ states. The O-2p bands are also split into p_x, p_y and p_z states. The calculated PBS of Cr-t_{2g} and O-2p states for the spin majority channel are represented in Figures 4 and 5 respectively. The formal valence of Cr in CrO_2 is +4 (Cr^{4+}), hence the number of available Cr-3d electrons is 2 (d^2). These two electrons are distributed among the three Cr- t_{2g} states, while both e_g states are found unoccupied. It is understandable from Figure 4 that d_{xy} state is fully occupied by a Cr-3d electron, shown in Figure 4(a), but the remaining single electron is equally shared by d_{yz} and d_{xz} states, shown in Figure 4(b). The electrons in these two states are delocalised and are found in the close vicinity of E_F. As a result, these two states (d_{yz} and d_{xz}) become exactly degenerate and orbital fluctuation between them is observed. The sharing of a single electron by these two degenerate t_{2g} states (d_{yz} and d_{xz}) is responsible for non-opening of a band gap near E_F. More interestingly, the occupied d_{xy} orbital is so directed towards O-2p states that p-d hybridisation is found to occur. The unfilled e_g states are shown in Figures 4(c) and 4(d). It is also obvious from Figure 5 that O-p_x and p_y states are exactly degenerate, as shown in Figure 5(a), states. All the three O-2p states (p_x, p_y and p_z) are hybridised with occupied Cr-3d_{xy} states. The hybridisations of p_x and p_y orbitals with Cr-d_{xy} orbital are stronger compared to Crd_{xy}-p_z hybridisation. Nevertheless, this p-d hybridisation is also accounted for the ferromagnetism of CrO_2.

Next concentration was devoted to carry out the PBS of Cr-3d and O-2p orbitals using U = 6 eV. Such higher value of U is applied for the better realisation of band structures. Figures 6 and 7 represent the PBS of Cr-3dt_{2g} and O-2p orbitals, respectively. It can be enunciated from Figure 6 that Cr-d_{xy} state is fully occupied; as it was observed in the absence of U, but this orbital is polarised well below E_F. The orbital fluctuations between d_{yz} and d_{xz} orbitals are now diminished. The correlation between the itinerant d-electrons in these two orbitals increases due to the presence of U. Due to the influence of strong on-site Coulomb repulsion U, d_{yz} and d_{xz} states split into bonding and anti-bonding components. The anti-bonding components of d_{yz} and d_{xz} states are found unoccupied and shift above E_F.

More interestingly, the bonding components of these two states become occupied and are shifted below E_F. Consequently, a band gap of E_g = 0.6 eV is opened near E_F. It is also observed in the PBS calculations that the two e_g states remain unfilled, which are shifted above E_F (not shown in figure). It is noteworthy from Table 1 that the total ground state energy of the present system gradually increases with U, which designates that the electrostatic repulsive force reduces with U. This result indicates that the electron correlation enhances progressively with U. Consequently, electron correlation plays a crucial role in the MIT of rutile CrO_2 at RT.

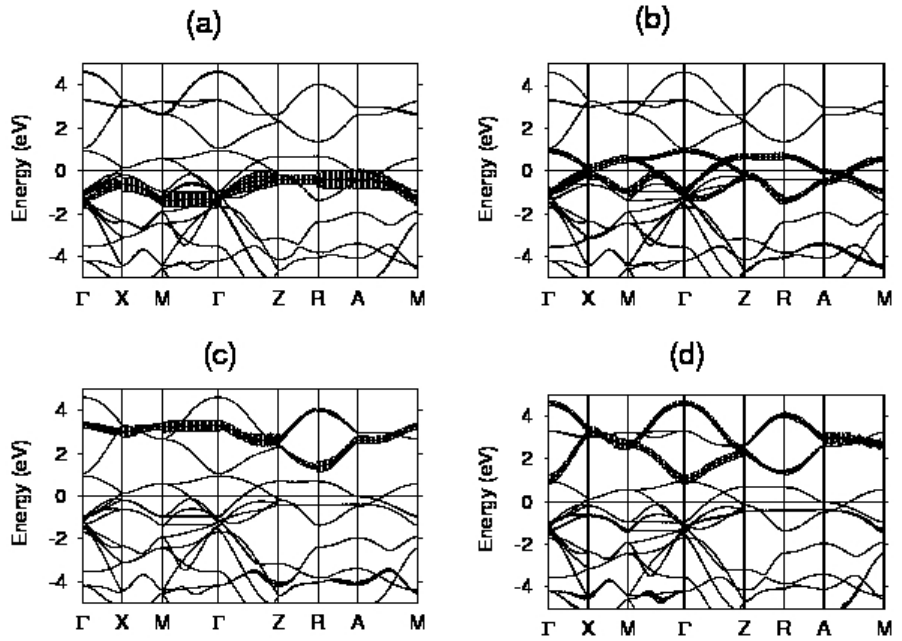

Figure 4: Calculated electronic band structures of (a) Cr-3d_{xy}, (b) $d_{yz/xz}$, (c) $d_{x^2-y^2}$, and (d) $d_{3z^2-r^2}$ states in the LSDA scheme. The Cr-3d_{xy} state is fully occupied by an electron but d_{yz} and d_{xz} states are partially occupied by the rest electron.

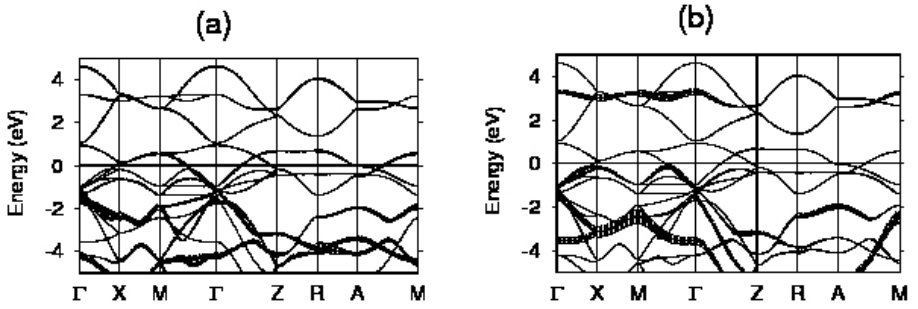

Figure 5: Electronic band structure of (a) O-2$p_{x/y}$, and (b) p_z states. The p_x and p_y states are degenerate states. All the three O-2p states are hybridised with occupied Cr-d_{xy} states.

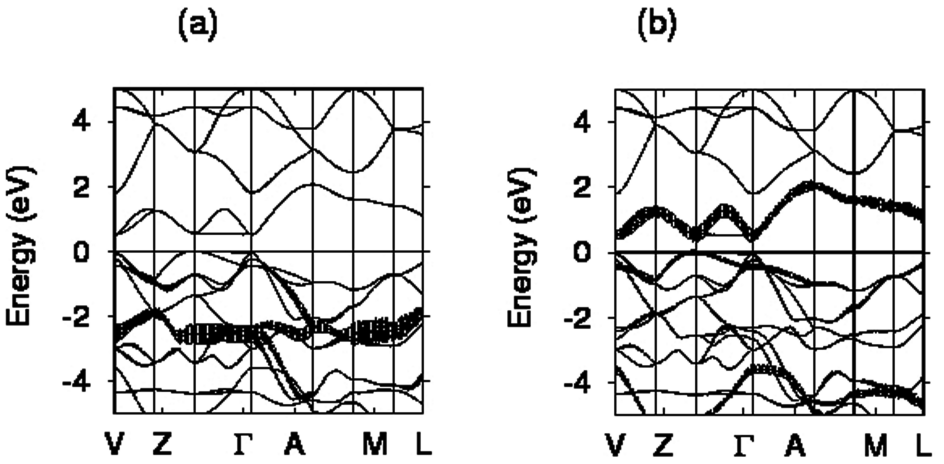

Figure 6: Calculated electronic band structure of (a) Cr-$d_{xy,}$ and (b) $d_{yz/xz}$ states in the LSDA+U scheme with U = 6 eV. The Cr-d_{xy} and the bonding components of d_{yz} and d_{xz} states are occupied. The antibonding components of d_{yz} and d_{xz} states are unoccupied.

It is further evident from the PBS calculations of O-2p states (Figure 7) that p_x and p_y states are degenerate and are strongly hybridised with the occupied bonding components of Cr-d_{yz} and d_{xz} states, wherein the p_z state is strongly hybridised with fully occupied Cr-d_{xy} state. Therefore, p-d hybridisations in the LSDA+U treatment enhance significantly compared to LSDA calculations. This result is also reflected in the magnetic moment calculations as reported in Table 1. It is noticeable from Table 1 that the Cr and O- magnetic moments increase with the augmentation of electron correlations. Interestingly, it is clear from the magnetic moment calculations that the O sites are anti-ferromagnetically coupled with Cr sites which are also responsible for p-d hybridisations.

Although for the application of U up to 4 eV, the electron correlation predominates but such electron correlation is not sufficient to split d_{yz} and d_{xz} into their constituent bonding and anti-bonding components. The electron in these two states still remains delocalised that is responsible for orbital fluctuations between these two states. Therefore, the single electron is still shared by the d_{yz} and d_{xz} states, resulting in metallic behaviour of rutile CrO_2. Nevertheless, applications of U increase spin polarisations for which the valence bands are shifted towards E_F and conduction bands are shifted away from E_F. The shifting of conduction bands is much higher in the spin minority channel compared to the spin majority channel, which is responsible for the broadening of semiconducting spin gaps (see Figure 2).

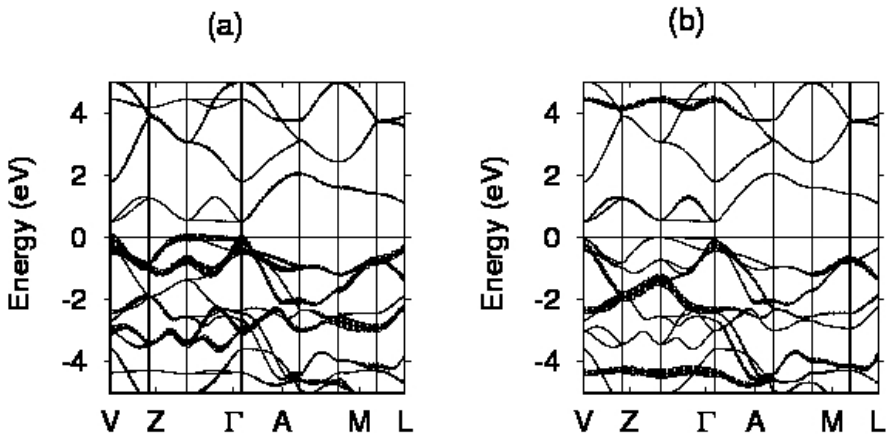

Figure 7: Electronic band structure of (a) O-2$p_{x/y}$, and (b) p_z states in the LSDA+U calculations with U = 6 eV. The O-2p_z state is hybridised with the occupied Cr-d_{xy} state, while p_x and p_y states are hybridised with the bonding components of Cr-d_{yz} and d_{xz} states.

3.3 Structural Properties

Finally, structural analyses have been performed across the MIT of rutile CrO_2. In this study, no structural transition was observed even in the applications of higher U values. The crystal structure and conventional Brillouin zone of rutile CrO_2 at RT are shown in Figure 8. Each Cr atom has six O-coordinations which form a CrO_6 octahedron. Every Cr site is placed at the centre of CrO_6 octahedron. It is emerged out from both LSDA and LSDA+U calculations that four neighbouring CrO_6 octahedra form a Cr-Cr rectangular four chain column in the ab plane. In each Cr-Cr rectangular four chain column, Cr atoms in the opposite diagonal positions ($z = 1$ or $z = 0$) lie in the same mirror plane, i.e., every mirror symmetry preserves by the Cr-atoms at the opposite diagonal positions, shown in Figure 8(b). The Cr-Cr distances in the rectangular four chain columns are uniform (=3.4503 (A°)). The measured Cr-O, Cr-Cr bond distances and <Cr-O-Cr, <O-Cr-O bond angles are reported in Table 3. All the Cr-Cr double chains have a uniform (2.9132 A°) bond distance which results in absence of lattice dimerisation within the crystal. Additionally, the uniform Cr-Cr distances in the Cr-Cr rectangular four-chain column is responsible for the non-formation of Cr-Cr tetramers. Consequently, the system remains in its three-dimensional structure. Therefore, no structural distortion within the crystal is observed; thereby the MIT in the rutile CrO_2 at RT structure exclusively triggers from the electron correlation effect.

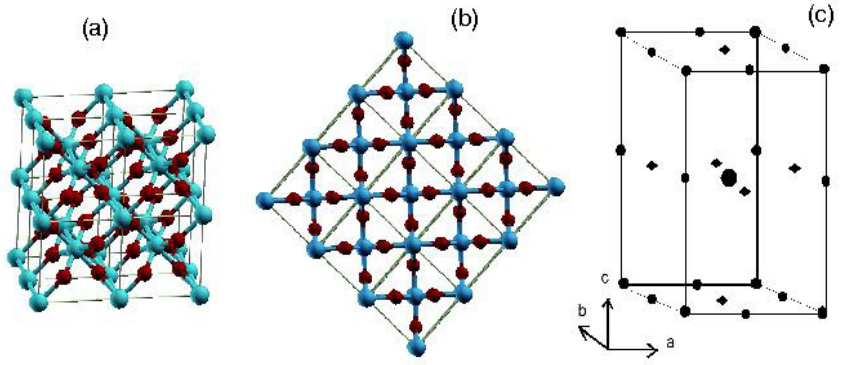

Figure 8: Ilustrations of (a) the crystal structure, (b) the rectangular four chain columns within the crystal, and (c) schematic representation of the Brillouin zone of CrO_2. The Cyan spheres represent Cr atoms and red spheres represent O atoms.

Table 3: Calculated Cr-O, Cr-Cr bond distances and <O-Cr-O, <Cr-O-Cr bond angles of CrO_2 in the rutile structure.

	Apical	Basal
Cr-O bond distances (A°)	1.9132 × 2	1.8886 × 4
Cr-Cr distances (A°)	2.9132	2.9132
<O-Cr-O angles (°)	180	90 × 2
<Cr-O-Cr angles (°)	130.33 × 2	130.33 × 2

It is further noted that all the <Cr-O-Cr bond angles are uniform (= 130.33°). The Cr-atoms within the Cr-Cr rectangular four chain columns are connected via O-atoms. These O atoms are anti-ferromagnetically coupled with Cr atoms (see Table 1) that leads to direct exchange interactions between Cr-t_{2g} and magnetically spin-polarised O-2p bands. These exchange interactions together with the conventional double exchange mechanism in the partially occupied Cr-t_{2g} bands are responsible for the ground state FM in the insulating CrO_2. Nevertheless, the exchange interactions between Cr-3dt_{2g} and O-2p orbitals enhance with the augmentation of U (see Table 1) due to an increase in the electron correlations.

4. CONCLUSION

In this study, it is observed that rutile CrO_2 is a half-metallic ferromagnet at RT. This compound is found metallic in the spin majority channel, while insulating in the spin minority channel with a semiconducting energy gap of ~ 1.85 eV.

In the spin majority channel, one of the available Cr-3d electrons fills Cr-d_{xy} state and the remaining single electron is equally shared by d_{yz} and d_{xz} states, causing the metallic behaviour of CrO_2. Double exchange interaction arising from strong Hund's coupling between partially occupied Cr-3dt_{2g} states is responsible for the ferromagnetism in CrO_2. Application of Coulomb interaction U increases correlations between the t_{2g} electrons which further increases spin polarisations. For the application of U = 1 to 4 eV, spin polarisation increases sequentially. The electrons in the conduction bands polarise away from E_F, whereas electrons in the valence bands polarise towards E_F, which is responsible for the shifting of these energy bands. The enhanced shifting of conduction bands in the spin minority channel is responsible for the widening of semiconducting spin gaps. Eventually, the application of U = 5 eV enables to open a band gap of 0.2 eV near E_F. It is observed that the d_{xy} state is occupied by a Cr-3d electron and is shifted well below E_F. This state is strongly hybridised with O-p_z state. The d_{yz} and d_{xz} states split into bonding and anti-bonding components under the influence of electron correlation effect. Both bonding components are occupied by the remaining single electron, whereas anti-bonding components are observed unfilled. These two bonding components are hybridised with O-p_x and p_y states. Further, occupied bonding components are downshifted and unoccupied anti-bonding components are shifted above E_F. Subsequently, a band gap of $E_g \sim 0.2$ eV is opened near E_F. Finally, double exchange interactions between the partially filled Cr-$d_{yz/xz}$ states together with p-d hybridisations are responsible for the FM behaviour of CrO_2 in the insulating phase.

5. ACKNOWLEDGEMENTS

I would like to express my sincere thanks and deep gratitude to Dr. Abhijit De, Head and Associate Professor, Department of Physics, Taki Govt. College, India for his valuable suggestions rendered for the betterment of the manuscript.

6. REFERENCES

1. Soulen, R. J. et al. (1998). Measuring the spin polarization of a metal with a superconducting point contact. *Sci.*, 282, 85–88, https://10.1126/science.282.5386.85.
2. Li, X. W., Gupta, A. & Xiao, G. (1999). Influence of strain on the magnetic properties of epitaxial (100) chromium dioxide (CrO_2) films. *Appl. Phys. Lett.*, 75, 713, https://doi.org/10.1063/1.124491.

3. Stagarescu, C. B. et al. (2000). The orbital character of O-2p unoccupied states near the Fermi level in CrO_2. *Phys. Rev. B*, 61, R9233, https://doi.org/10.1103/PhysRevB.61.R9233.
4. Fang, F. Y. et al. (2000). Uniaxial anisotropy and switching behavior in epitaxial CrO_2 films. *Appl. Phys. Lett.*, 77, 286, https://doi.org/10.1063/1.126952.
5. Ji, Y. et al. (2001). Determination of the spin polarization of half-metallic CrO_2 by point contact Andreev reflection. *Phys. Rev. Lett.*, 86, 5585, https://doi.org/10.1103/PhysRevLett.86.5585.
6. Korotin, M. A. et al. (1998). CrO_2: A self-doped double exchange ferromagnet. *Phys. Rev. Lett.*, 80, 4305, https://doi.org/10.1103/PhysRevLett.80.4305.
7. Mazin, I. I. et al. (1999). Transport, optical, and electronic properties of the half-metal CrO_2. *Phys. Rev. B*, 59, 411, https://doi.org/10.1103/PhysRevB.59.411.
8. Kunes, J. et al. (2002). Electronic structure of CrO_2 as deduced from its magneto-optical Kerr spectra. *Phys. Rev. B*, 65, 165105, https://doi.org/10.1103/PhysRevB.65.165105.
9. Toropova, A. & Kotliar, G. (2005). Electronic structure and magnetic anisotropy of CrO_2. *Phys. Rev. B*, 71, 172403, https://doi.org/10.1103/PhysRevB.71.172403.
10. Dedkov, Y. S. et al. (2005). Correlations in the electronic structure of half-metallic ferromagnetic CrO_2 films: An x-ray absorption and resonant photoemission spectroscopy study. *Phys. Rev. B*, 72, 060401(R), https://doi.org/10.1103/PhysRevB.72.060401.
11. Kanchana, V. et al. (2006). Calculated electronic structure and x-ray magnetic circular dichroism of CrO_2. *J. Phys. Condens. Matter.*, 18, 5155, https://doi.org/10.1088/0953-8984/18/22/015.
12. Singh, G. P. et al. (2009). Synthesis and morphological stability in CrO_2 single crystals of a half-metallic ferromagnetic compound. *J. Phys. Conf. Series*, 144, 012110, https://doi.org/10.1088/1742-6596/144/1/012110.
13. Anwar, M. S. et al. (2010). Long-range supercurrents through half-metallic ferromagnetic CrO_2. *Phys. Rev. B*, 82, 100501(R), http://doi.org/10.1103/PhysRevB.82.100501.
14. Wu, H. Y. et al. (2012). Electronic and elastic properties of CrO_2 in the orthorhombic $CaCl_2$-type structure. *Int. J. Mod. Phys. B*, 15, 1250091, https://doi.org/10.1142/S0217979212500919.
15. Singh, A. et al. (2015). Colossal proximity effect in a superconducting triplet spin valve based on the half-metallic ferromagnet CrO_2. *Phys. Rev. X*, 5, 021019, https://doi.org/10.1103/PhysRevX.5.021019.
16. Moodera, J. S. et al. (1995). Large magnetoresistance at room temperature in ferromagnetic thin film tunnel junctions *Phys. Rev. Lett.*, 74, 3273, https://doi.org/10.1103/PhysRevLett.74.3273.
17. Gallagher, W. J. et al. (1997). Microstructured magnetic tunnel junctions. *J. Appl. Phys.*, 81, 3741, https://doi.org/10.1063/1.364744.
18. Boeve, H., Boeck, J. D. & Borghs, G. (2001). Low-resistance magnetic tunnel junctions by in-situ natural oxidation. *J. Appl. Phys.*, 89, 482, https://doi.org/10.1063/1.1328064.

19. Gupta, A., Li, X. W. & Xiao, G. (2001). Inverse magnetoresistance in chromium-dioxide-based magnetic tunnel junctions. *Appl. Phys. Lett*., 78, 1894, https://doi.org/10.1063/1.1356726.
20. Dai, J. & Tang, J. (2001). Junction-like magnetoresistance of intergranular tunneling in field-aligned chromium dioxide powders. *Phys. Rev. B*, 63, 054434, https://doi.org/10.1103/PhysRevB.63.054434.
21. Hwang, H. Y. et al. (1996). Spin-polarized intergrain tunneling in $La_{2/3}Sr_{1/3}MnO_3$. *Phys. Rev. Lett*., 77, 2041, https://doi.org/10.1103/PhysRevLett.77.2041.
22. Manoharan, S. S. et al. (1998). Extrinsic giant magnetoresistance in chromium (IV) oxide, CrO_2. *Appl. Phys. Lett.*, 72, 984, https://doi.org/10.1063/1.120616.
23. Hohenberg, P. & Kohn, W. (1964). Inhomogeneous electron gas. *Phys. Rev. B*, 136, 864, https://doi.org/10.1103/PhysRev.136.B864.
24. Kohn, W. & Sham, L. J. (1965). Self-consistent equations including exchange and correlation effects. *Phys. Rev. A*, 140, 1133, https://doi.org/10.1103/PhysRev.140.A1133.
25. Jepsen, O. & Andersen, O. K. (2000). The STUTTGART TB-LMTO program, version 47. Retrieved 10 January 2017 from https://www2.fkf.mpg.de/andersen/LMTODOC/LMTODOC.html.
26. Anderson, O. K. (1975). Linear methods in band theory. *Phys. Rev. B*, 12, 3060, https://doi.org/10.1103/PhysRevB.12.3060.
27. Anderson, O. K. & Jepsen, O. (1984). Explicit, first-principles tight-binding theory. *Phys. Rev. Lett.*, 53, 2571, https://doi.org/10.1103/PhysRevLett.53.2571.
28. Perdew, J. P. & Wang, Y. (1992). Accurate and simple analytic representation of the electron-gas correlation energy. *Phys. Rev. B*, 45, 13244, https://doi.org/10.1103/PhysRevB.45.13244.
29. Coey, J. M. D. & Venkatesan, M. (2002*)*. Half-metallic ferromagnetism: Example of CrO_2. *J. Appl. Phys.*, 91(10), 8345–8350, https://doi.org/10.1063/1.1447879.
30. Kim, S. et al. (2012). Pressure-induced phonon softenings and the structural and magnetic transitions in CrO_2. *Phys. Rev. B*, *85*, 094106, https://doi.org/10.1103/PhysRevB.85.094106.
31. Biswas, S. (2018). Metal-insulator transition in the high pressure cubic CaF_2-type structure of CrO_2. *Bull. Mater. Sci.*, 41, 33, https://doi.org/10.1007/s12034-018-1551-0.
32. Biswas, S. (2018). Charge ordering in the metal-insulator transition of V-doped CrO_2 in the rutile structure. *J. Mol. Mod.*, 24, 111, https://doi.org/10.1007/s00894-018-3647-2.